

Terahertz molecular imaging for medical diagnosis

Seung Jae Oh¹, Yong-Min Huh¹, Seungjoo Haam², #Jin-suck Suh¹, #Joo-Hiuk Son³

¹Department of Radiology, YUMS-KRIBB Medical Convergence Center, Severance Biomedical Science Institute, College of Medicine, Yonsei University, Seoul 120-749, Republic of Korea, jss@yuhs.ac

²Department of Chemical & Biomolecular Engineering, Yonsei University, Seoul 120-752, Republic of Korea

³Laboratory for Terahertz Biophotonics, Department of Physics, University of Seoul, Seoul 130-743, Republic of Korea, joohiuk@uos.ac.kr

Abstract

We present the principle of terahertz molecular imaging (TMI) technique using nanoparticle probes. We obtained the diagnostic images of cancerous tumors *ex vivo* and *in vivo* in the preclinical stage. The results of our study prove that TMI is feasible for medical diagnosis at the clinical stage.

Keywords : Terahertz Molecular Imaging Nanoprobes

1. Introduction

The conventional terahertz (THz) imaging technique for medical diagnosis has measured the differences in the interstitial water contents or the structural change between normal and abnormal regions can be measured. However, miniscule differences at the molecular and cellular levels, such as the differences between benign and malignant tumors, have not been conclusively identified by employing the THz imaging technique [1]. The sensitivity of THz imaging can be improved by using nanoprobe that have been used in magnetic resonance imaging and optical molecular imaging techniques [2-5]. In this paper, we present a novel THz molecular imaging (TMI) technique in which THz electromagnetic waves and gold nanorods (GNRs) used as nanoparticle probes (nanoprobes) are employed, with the operating principle, as shown in Fig. 1. We also present the diagnostic TMI images of livers, spleens, kidney, and epithelial cancers in mice *ex vivo* and *in vivo* as examples of images obtained by the TMI technique. Furthermore, in order to evaluate the application of the technique in a potential medical-diagnosis imaging system, we discuss the sensitivity and quantification of this technique, and the resolution of the images obtained using the technique.

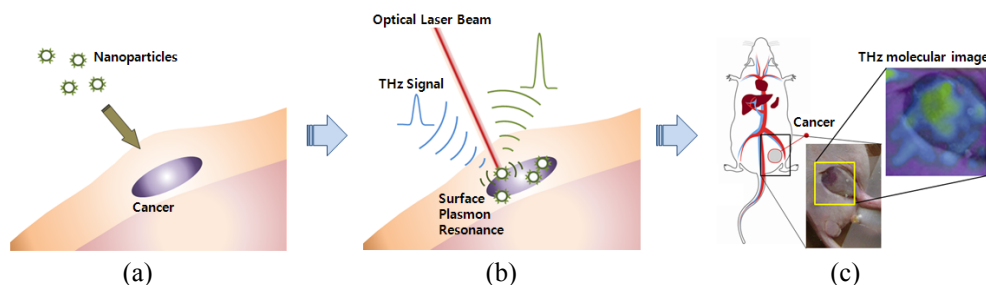


Figure 1: (a) Targeting of tumors by antibody-conjugated nanoparticles, (b) differential THz detection under the modulation of surface plasmons, and (c) *in vivo* terahertz molecular imaging.

2. Theory and Measurements

TMI was performed by measuring the change in the THz signal caused by surface plasmon polaritons (SPPs) produced on the surface of metallic nanoprobe under the illumination of a near-infrared (NIR) beam. The optically generated SPPs converted most of their energy into heat around

the surface of nanoprobes and increased the temperature of the media surrounding the nanoprobes. THz waves were used to monitor the increase in temperature. The temperature sensitivity of THz waves in water is considerably higher than those of NIR or visible waves [6,7]. Thus, the TMI technique can be employed to obtain precise images of the distribution of minute quantities of nanoprobes by measuring the temperature around the nanoprobes.

The TMI signals from a sample with nanoprobes could be modulated by altering the intensities or duty ratios of NIR beams, as shown Fig. 2. The modulated NIR beam changed the THz signals because it altered the temperature of water surrounding the nanoprobes. However, in the absence of GNRs or NIR beam irradiation, the THz signals showed little change. The THz signal modulated by the NIR beam was used to obtain THz images of the nanoprobes. By employing this differential THz detection technique, a high-contrast THz image could be obtained because the signals were produced only from the nanoprobes and the THz waves had high sensitivity.

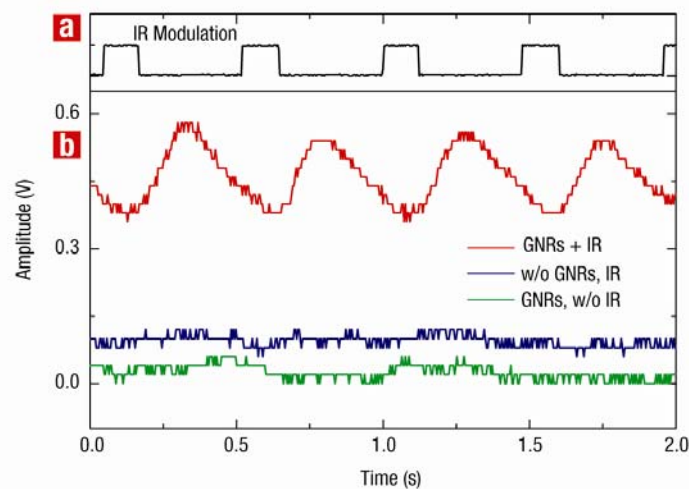


Figure 2: THz response under NIR modulation. Panel (a) shows the NIR signal modulated by using a mechanical shutter (black line). Panel (b) shows the THz responses of water using GNRs under NIR irradiation (red line), GNRs without NIR irradiation (green line), and without GNRs under NIR irradiation (blue line). The power of the NIR beam was 15 W/cm^2 and the diameters of the THz and NIR beams were 0.8 mm. The concentration of the GNR solution was $100 \mu\text{M}$. The time-dependent THz signals were observed using an oscilloscope triggered by the modulation signal of the NIR beam [3].

As shown in Fig. 3, the TMI system consisted of two parts: a 808 nm continuous-wave (CW) NIR laser for inducing SPP resonance and the reflection-mode THz imaging system for monitoring laser-induced temperature changes in samples. The THz pulses generated on a InAs semiconductor wafer were measured by a low-temperature-grown (LT)-GaAs antenna using a fast optical delay line that vibrated at a frequency of 20 Hz and a span of 36 ps. The diameter of the THz beam focused on the sample was 0.8 mm, and an NIR laser beam with the same diameter was also focused on the sample, thus overlapping with the THz beam. The THz imaging system, excluding the sample, was constructed within a dry box so that the produced THz signals would not be affected by humidity.

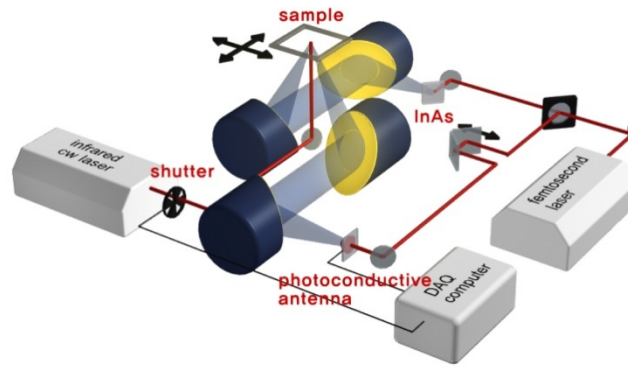


Figure 3: THz molecular imaging system consisting of a reflection-mode THz imaging setup and an NIR laser [3].

The GNRs, which we used as nanoprobe, were fabricated by a seed-mediated growth technique. The GNRs were coated with polyethylene glycol (PEG) and modified by Cetuximab (CET), which specifically targets only the cancer cells in which epidermal growth factor receptors (EGFRs) are highly developed. Thus, Cetuximab-PEGylated gold nanorods (CET-PGNRs) were synthesized and used as the nanoprobe in this study. For an animal experiment, we prepared several tens of xenograft mouse models. A431 cells were injected subcutaneously in the proximal thigh region of male BALB/c-nude mice that were 5–8 weeks old; these mice were obtained from the Institute of Medical Science (University of Tokyo). All experiments were conducted with the approval of the Association for Assessment and Accreditation of Laboratory Animal Care (AAALAC) International.

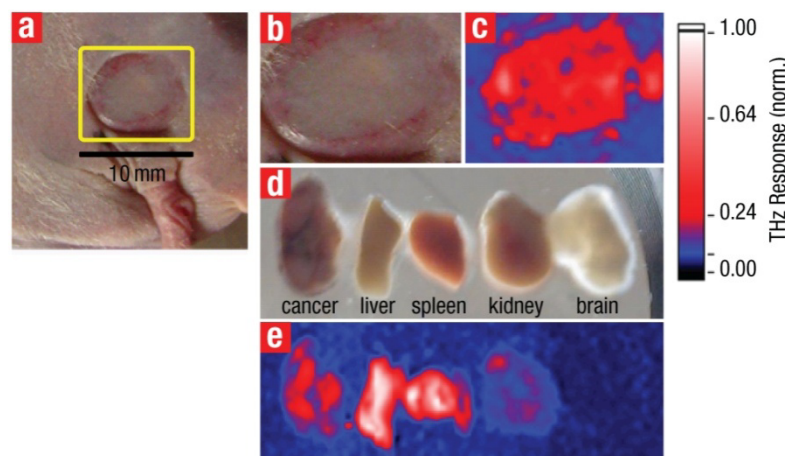


Figure 4: *In vivo* and *ex vivo* THz molecular images of tumors. (a) and (b) show visible images of the mouse with an A431 tumor (size = 2.1 cm³). (c) shows the THz molecular image of (b). (d) shows the visible images of the tumor, liver, spleen, kidney, and brain. (e) shows the THz molecular image of (d). The power of the NIR beam was 80 W/cm² and the diameters of the THz and NIR beams were 0.8 mm. The image was obtained with a scan step of 250 μm and a time delay of 3 s per pixel, 24 h after the injection of 100 μL of CET-PGNRs at a concentration of 1 mM [3].

We obtained the *in vivo* diagnostic images of cancerous tumors by the TMI technique. A xenograft mouse model bearing the A431 epidermoid carcinoma tumor (Figs. 4(a) and (b)) was prepared and the nanoprobe with 100 μL of CET-PGNRs at a concentration of 1 mM were injected into the mouse through the tail vein. All the images of the cancerous tumor were captured 24 h after injection, as shown in Fig. 4. Although the visual image (Fig. 4(b)) showed only a superficial shape of tumors on the skin, a high-contrast THz image revealed the location and size of the tumor with

nanoprobes. After obtaining the *in vivo* images, we killed the mouse injected with nanoprobes and showed that the nanoprobes were delivered well to specific organs. The tumor, liver, spleen, kidney, and brain were surgically extracted (Fig. 4(d)). Figure 4(e) shows the TMI images of these organs. The amplitudes of the TMI images of the tumor, liver, and spleen were higher than those of the brain and kidney, although the brightness of the THz images of all of the organs extracted from a mouse which was not injected with CET-PGNRs were almost identical. This showed that the circulation system of the mouse delivered the nanoprobes into the targeted tumor and some of the nanoprobes were deposited at by the liver and spleen on the way to the tumor. The results of our study show that TMI is sufficiently sensitive for identifying the different parts or organs targeted by the nanoprobes.

3. Conclusion

We demonstrated medical diagnosis by employing the TMI technique with nanoprobes and obtained *ex vivo* and *in vivo* target-specific high-contrast images of A431 cancerous tumors noninvasively with high sensitivity. Thus, this technique facilitates the early diagnosis of cancers, and it is also capable of monitoring drug delivery processes and identifying the minute differences at a cellular level.

References

- [1] J. -H. Son, "Terahertz Electromagnetic Interactions with Biological Matter and Their Applications," *J. Appl. Phys.*, vol. 105, pp. 102033 1-10, 2009.
- [2] S. J. Oh, J. Kang, I. Maeng, J.-S. Suh, Y.-M. Huh, S. Haam, J.-H. Son, "Nanoparticle-enabled Terahertz Imaging for Cancer Diagnosis," *Opt. Express*, vol. 17, pp. 3469-3475, 2009.
- [3] S. J. Oh, J. Choi, I. Maeng, J. Y. Park, K. Lee, Y.-M. Huh, J.-S. Suh, S. Haam, J.-H. Son, "Molecular Imaging with Terahertz Waves," *Opt. Express*, vol. 19, pp. 4009-4016, 2011.
- [4] J. -H. Lee, Y. -M. Huh, Y. -W. Jun, J. -W. Seo, J. -T. Jang, H. -T. Song, S. Kim, E. -J. Cho, H. -G. Yoon, J. -S. Suh, J. Chen, "Artificially Engineered Magnetic Nanoparticles for Ultra-sensitive Molecular Imaging," *Nature Medicine*, vol. 13, pp. 95-99, 2006.
- [5] J. Lee, J. Yang, H. Ko, S. J. Oh, J. Kang, J. -H. Son, K. Lee, S. -W. Lee, H. -G. Yoon, J. -S. Suh, Y. -M. Huh, S. Haam, "Multifunctional Magnetic Gold Nanocomposites: Human Epithelial Cancer Detection via Magnetic Resonance Imaging and Localized Synchronous Therapy," *Adv. Func. Mat.*, vol. 18, pp. 258-264, 2008.
- [6] C. Rønne, L. Thrane, P. Åstrand, A. Wallqvist, K. V. Mikkelsen, S. R. Keiding, "Investigation of the Temperature Dependence of Dielectric Relaxation in Liquid Water by THz Reflection Spectroscopy and Molecular Dynamics Simulation," *J. of Chem. and Phys.*, vol. 107, pp. 5319-5331, 1997.
- [7] J. R. Collins, "Change in the Infra-red Absorption Spectrum of Water with Temperature," *Phys. Rev.*, vol. 26, pp. 771-779, 1925.

Acknowledgments

This study was supported by a grant from the Korean Health Technology R&D Project of the Ministry for Health, Welfare & Family Affairs, Republic of Korea (A101954) and a National Research Foundation of Korea (NRF) grant (20100020647, 20100001979, 20100015989, 20100011934, 20090054519) funded by the Korean government (MEST).